NASA TECHNICAL NOTE

NASA TN D-4210

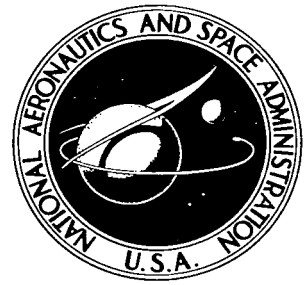

NASA TN D-4210

AN INVESTIGATION OF THE USE OF ACOUSTIC ENERGY ABSORBERS TO DAMP LOX/RP-1 COMBUSTION OSCILLATIONS

by Curtis R. Bailey

George C. Marshall Space Flight Center
Huntsville, Ala.

NATIONAL AERONAUTICS AND SPACE ADMINISTRATION • WASHINGTON, D. C. • NOVEMBER 1967

NASA TN D-4210

AN INVESTIGATION OF THE USE OF ACOUSTIC ENERGY ABSORBERS TO DAMP LOX/RP-1 COMBUSTION OSCILLATIONS

By Curtis R. Bailey

George C. Marshall Space Flight Center
Huntsville, Ala.

NATIONAL AERONAUTICS AND SPACE ADMINISTRATION

For sale by the Clearinghouse for Federal Scientific and Technical Information
Springfield, Virginia 22151 – CFSTI price $3.00

TABLE OF CONTENTS

LIST OF TABLES

LIST OF ILLUSTRATIONS

DEFINITION OF SYMBOLS

Symbol	Definition
A_f	Amplitude Parameter
A_t	Nozzle Throat Area
C	Sonic Velocity
C*	Characteristic Velocity
D	Diameter
F	Thrust
g	Acceleration Due to Gravity
L	Liner Backing Distance
L*	Characteristic Chamber Length
ℓ_{ef}	Effective Aperture Length
P_i	Incident Pressure Amplitude
Q	Quality Factor
R_d	Liner Aperture Resistance
T	Temperature
t	Test Duration or Liner Thickness
W	Flow Rate
X_o	Particle Displacement
α	Absorption Coefficient
Δ	Differential
ϵ	Nonlinear Resistance Term
η	Efficiency
θ	Specific Input Resistance
μ	Viscosity
ρ	Density
σ	Open Area Ratio
ω	Frequency

DEFINITION OF SYMBOLS (Concluded)

Subscripts

Symbol	Definition
a	Liner Apertures
c	Combustion Chamber
f	Fuel
o	Aperture Resonance or Oxidizer
t	First Tangential
v	With Flow
1	Liner Cavity, Injector End
2	Liner Cavity, Nozzle End

AN INVESTIGATION OF THE USE OF ACOUSTIC ENERGY ABSORBERS TO DAMP LOX/RP-1 COMBUSTION OSCILLATIONS

By

Curtis R. Bailey

SUMMARY

The effectiveness of acoustic energy absorbers in damping LOX/RP-1 combustion oscillations was investigated. Test firings were conducted using both cooled and uncooled absorbers in a 4000-pound thrust combustion chamber. Combustion oscillations, which had been consistently severe without the liners, were effectively damped when the liners were installed. Oscillations resulting from bomb-induced disturbances within the chamber were also effectively damped. A liner one-half as long as the combustion chamber and positioned at the injector end was as effective as the full-length liner.

A sample absorber calculation is presented and absorber design procedures are outlined. The effects of variations in design assumptions are discussed, and it is concluded that these effects, plus the lack of a proven design procedure, preclude the accurate calculation of the absorption coefficient.

INTRODUCTION

Acoustic energy absorbers have appeared attractive for several years as a means of eliminating combustion instability in rocket engine thrust chambers. Since 1963, a NASA sponsored program, NAS8-11038 "A Study of the Suppression of Combustion Oscillations with Mechanical Damping Devices," has been conducted by Pratt and Whitney Aircraft for the purpose of defining and optimizing a usable theory of absorber design for use in rocket thrust chambers. The use of a perforated combustion chamber liner having an outer shell that forms a parallel array of Helmholtz resonators was explored. These liners or absorbers have been very effective in damping combustion oscillations.

The subject program was initiated to investigate the performance of acoustic energy absorbers in a liquid oxygen/RP-1 combustor in which the instability was both severe and repeatable. Specifically, the program goals were to

determine; (a) the theoretical absorption coefficient required to damp the instability, (b) the sensitivity of absorber location within the combustion chamber, (c) the effects of bomb-induced disturbances on combustion stability, and (d) determination of cooling requirements for the liner cavity shell.

The author acknowledges the efforts of the Advanced Technology Test Section, George C. Marshall Space Flight Center, in executing this program, and the service of Mr. B. F. Boggs, Rocketdyne Division, North American Aviation, Inc., for providing the bombs used in the stability rating tests. A special thanks goes to Mr. G. D. Garrison, Pratt and Whitney Aircraft, for his many and varied contributions to this effort.

TEST CONFIGURATION

The basic thrust chamber configuration shown in Figure 1(a) used liquid oxygen and RP-1 propellants and produced a nominal thrust of 4000 pounds at a chamber pressure of 1000 psia. The chamber had a characteristic length (L*) of 47.5 inches and a nozzle contraction ratio of 4.5. The injector was of concentric tube design with oxidizer in the center tube. The design used 152 stainless steel, 0.063 OD, 0.043 ID oxidizer tubes, with 0.070-inch fuel orificies. The nozzle and chamber sections were made of copper, and the injector assembly was stainless steel.

The test configuration, modified to accomodate the cooled acoustic liner, is shown in Figure 1(b). Basic chamber dimensions are the same as for the chamber shown in Figure 1(a). Installation of the uncooled acoustic liner was similar. The cooled and uncooled liners are shown in Figure 2. The uncooled liner was made of stainless steel coated with 0.020-inch thick zirconia. Open area ratio of the liner was 2.3 percent, provided by 1700 - 0.040-inch diameter holes. Liner and resonator cavity thicknesses were 0.10 inches each. The water-cooled liner consisted of fifty 0.25-inch OD, 0.040-inch wall stainless steel tubes welded together to form a 3.73-inch diameter chamber. Thirteen hundred and fifty 0.040-inch holes were drilled between the tubes providing a full-length liner as shown in Figure 2(c). After several tests had been conducted, a half-length liner was obtained by welding the apertures closed in the downstream half of the chamber. Liner open area ratio was 2.5 percent. Resonator cavity thickness was normally 0.169 inches, but half-cylinder inserts were added during the test phase to reduce it to 0.072 inches.

The solid propellant charges or bombs used for the stability rating tests were enclosed in an ablative case that was screwed onto the injector face approximately 0.70 inches from the chamber wall. Installation of the bomb required the removal of one of the injector elements. The charges contained either a 6.9 grain Olin Matheson blasting cap or a 13.5 grain Du Pont E-83 blasting cap that ignited when the case ablated away.

INSTRUMENTATION AND DATA REDUCTION

Instrumentation was provided for all measurements required to determine thrust chamber performance and facility operation. All facility and low-frequency thrust chamber measurements were recorded on System Engineering Laboratories (SEL) and Scientific Data Systems (SDS) digital instrumentation systems and Consolidated Electrodynamics Corporation (CEC) oscillographs. Fluid flow measurements were made with Potter turbine flowmeters, and steady state pressure measurements were made using either Wianko variable reluctance transducers or CEC strain gage transducers. Flow measurement accuracy was approximately ± 1.5 percent and steady-state pressure measurement accuracy was approximately ± 1.0 percent. Liner cavity gas temperatures were measured with chromel-alumel thermocouples positioned as shown in Figure 2(c). Overall measurement accuracy was approximately ± 1.5 percent.

All high frequency data were recorded and stored by an Ampex tape recorder and later transferred to a CEC oscillograph. The chamber pressure data were digitized at a sampling rate of 20,000 samples per second, then analyzed using an IBM 7094 random vibration analysis program. The data were usually processed with a 20 cycles per second filter over a total band width of 10,000 cycles per second, then presented by an automatic digital plotter in the form of rms pressure as a function of frequency.

Several types of transducers were used for transient chamber pressure measurements, and significantly different results were obtained during instability, depending on which transducer was used and how it was installed. Photocon model 352A transducers recessed approximately 0.10 inches from the liner wall were used for the uncooled liner firings and satisfactorily provided amplitude measurements accurate (± 10 percent) to frequencies approaching 10,000 cps. A base instability firing, 147-25, in which a liner was not used was monitored with a Dynisco PT-49 mounted flush with the chamber wall approximately one inch from the injector face. This configuration provided measurements accurate

(± 10 percent) to 10,000 cps, but it was not suitable for continued use, because it could not withstand the high heating rates encountered during instability. Aerojet helium bleed transducers, model HB-3X and HB-4X, were used exclusively for the cooled liner test series, and an HB-4X was used with a Dynisco PT-130 to monitor a second base instability firing, 176-12. The PT-130 was recessed one-half inch from the inner wall of the chamber and connected to the chamber with five 1/8-inch diameter holes. Resonance is reached with this configuration at approximately 3000 cps and amplitude measurement accuracy above 2000 cps is questionable. For this application, the response of the helium bleed transducers was limited to approximately 5000 cps. The effect of this was not particularly important, however, because all liner firings were stable. For the one unstable firing using a helium bleed transducer, 176-12, the measured amplitudes are not accurate.

TEST RESULTS

Basic Thrust Chamber

Typical combustion instability data obtained during firings of the unlined chamber in a previous test program are presented in Figures 3 and 4. Figure 3 shows the peak-to-peak amplitude of chamber pressure as presented by a digital plotter, and Figure 4 is a frequency analysis of the same data. Note that peak-to-peak amplitude is approximately 1600 psi, and the predominate frequency is 7200 cps. This corresponds to the first tangential acoustic mode of the chamber. The thrust chamber configuration shown in Figure 1(a) consistently produced this type of instability in firings conducted in another program. For mixture ratios (O/F) greater than 1.5, a 100 cps chugging mode started immediately after ignition with the first tangential mode gradually becoming predominate after approximately one second. For mixture ratios less than 1.0, the chugging persisted throughout the run with no high frequency instability.

Uncooled Acoustic Liner

Two firings used the uncooled liner shown in Figure 2(a). This design had a calculated absorption coefficient of approximately 95 percent at 7200 cps, the first tangential frequency. The design assumptions and their effects will be discussed later. There was no instability during either firing. A comparison of Figures 4 and 5 illustrates how effectively the instability was damped. The uncooled liners were unable to withstand the high heating rates for even short duration firings, and it was necessary to design a cooled configuration. Figure 6 shows the condition of an uncooled liner after one three-second firing.

Cooled Acoustic Liner

Tests number 176-1 through 176-4 were conducted using the full-length cooled liner installed without the cavity spacers so that backing cavity depth was 0.169 inches. Basic test results are presented in Table I. The oscillogram of the pressures measured during run 176-4 is presented at the top of Figure 7, and the traces are typical of the other firings. The liner damped all instability.

Backing cavity spacers were installed in the liner prior to run 176-5, reducing the backing cavity depth to 0.072 inches. The test results showed no change in performance with this configuration, and the combustion remained stable.

Prior to run 176-6 all liner apertures in the downstream half of the chamber were welded closed. The backing spacers were also removed to provide the original backing cavity depth. Run 176-6 was aborted due to a TEA inlet pin failure, but runs 176-7 and 176-8 used the same configuration for run durations of five seconds and three seconds, respectively. No detectable difference was noted between the stability obtained with this configuration and the previous ones.

Run 176-9 used the concentric orifice injector modified to accept the ablative-type pulse charge. The 6.9-grain charge used caused a 300 psi pulse. The pulse was not as spontaneous as expected with a rise time of 1.5 milliseconds. The pulse developed into 100 psi peak-to-peak, 6400 cps oscillations that damped out completely in 45 milliseconds.

Run 176-10 used the same configuration as the previous test, except the cavity spacers were again inserted in the backing cavity. The 6.9 grain charge was also used for this firing, but the oscillograph traces indicated that the charge burned erratically. Several small pressure surges were recorded but no significant sharp pulses. There was no instability.

The last firing with the acoustic liner, run 176-11, used the same configuration as the previous test except a 13.5 grain pulse charge was used. Figure 8 shows a trace of the 2600 psi pulse which resulted. As shown, there was no combustion instability. The high overpressure yielded the liner somewhat, although the damage was not extensive.

The final firing, run 176-12, used no acoustic liner and was made to obtain additional instability characteristics of the configuration. The combustion was characteristically unstable. An oscillagram of the pressure traces is shown at the bottom of Figure 7. For reasons previously discussed in the instrumentation section, the pressure amplitudes are not accurate and are, therefore, not presented.

DESIGN CONSIDERATIONS

Before any attempt is made to draw conclusions based on the test results, the liner design assumptions will be discussed and consideration will be given to the variations in absorption coefficients which result. Unfortunately, no method exists by which absorption coefficients can be measured during thrust chamber firings, and the instability data must be analyzed as functions of calculated absorption coefficients. Since the values of the coefficients can vary significantly with combustor operating conditions not measured in this program, a discussion of the effects of these variables is considered necessary. Also, it should be made clear that the acoustic energy absorber design theory is still in a state of development, and the effects of some of the conditions present in rocket thrust chambers have not been resolved. The effects on this program of some of these unknowns are discussed below.

Uncooled Acoustic Liner

Calculated values of absorption coefficients for the uncooled liners are plotted as functions of frequency and aperture gas temperature in Figure 9. The assumed aperture gas temperature was 3000 °R and, since the available velocity correction procedures were not believed to be accurate, zero gas velocity past the apertures was assumed. Theoretical absorption for the liner at design conditions is shown as the top curve for the no-flow cases on Figure 9. Note that the absorption coefficient is approximately 94 percent at 7200 cps, the unstable frequency, with the curve remaining fairly flat over the entire band. For the assumed no-flow conditions, note also the effect if the assumed temperature was too high. At 2000 °R, the absorption coefficient drops to 16 percent and at 1000 °R it is essentially zero. Consider now the effects of a faulty assumption of zero gas velocity past the liner. Absorption coefficient curves for velocities of 250 ft/sec and 500 ft/sec are also presented in Figure 9. Note that the effect of gas temperature is reversed from the no-flow case, with lower temperatures producing higher values of absorption coefficients.

Cooled Acoustic Liner

Data of the same type for the cooled acoustic liners are presented in Figures 10 and 11. For these liners, the assumed aperture gas temperature was 3000 °R with a gas velocity of 500 ft/sec past the liner. At these conditions, theoretical absorption coefficient at design frequency was 80 percent for the 0.169-inch cavity liner. The addition of backing spacers to reduce cavity depth to 0.072 inches reduced the design absorption coefficient to approximately 20 percent, as shown in Figure 11. As an aid to demonstrate the effects of design assumptions, the frequency

variable was removed and the absorption coefficients at 7200 cps were plotted in Figure 12 as functions of velocity and gas temperature.

Sound Pressure Level Effects

Presented in the Appendix are sample calculations of absorption coefficients of the acoustic liners used in this program. Note that one of the design assumptions is the incident pressure amplitude of 190 db or 1872 lbf/ft^2. Ideally, this pressure amplitude should correspond to that caused by the energy input per cycle of the instability. This amplitude cannot be measured, however, and the designer must assume a reasonable value. In most thrust chambers, instability builds up gradually and 190 db would be a reasonable assumption for the pressure increase per cycle. This was assumed to be the case with the subject thrust chamber. An actual value lower than this should be of no consequence, because an amplitude of 190 db would be reached in subsequent cycles. An actual value much higher than this was not considered probable and could not be used in design calculations, because 190 db is considered to be the current limit of the technology.

Nonliner Resistance Effects

As sound pressure amplitudes become greater than approximately 100 db, increased gas turbulence in the liner apertures adds a nonlinear resistance (ϵ) to the total acoustic resistance. This nonlinear resistance has been the subject of considerable work and is extensively discussed in References 1 through 5. It should suffice here to say that accurate prediction of the nonlinear resistance effects has not been demonstrated. In fact, it has not yet been shown conclusively whether ϵ is a prime function of incident sound pressure level or whether it is more accurately a function of the ratio of particle displacement in the aperture to the aperture thickness. Data published by the authorities referenced above are presented in Figure 13. The nonlinear resistances used in this program were obtained primarily from the Blackman correlation based on particle displacement ratio. All absorption coefficient data presented and discussed to this point have been based on this correlation. Information recently made available in Reference 4 indicates that a correlation which is possibly more accurate is the Pratt and Whitney curve based on incident sound pressure level. Figures 14 and 15 show the effects of the design assumptions if the cooled liner absorption coefficients are recalculated based on this correlation. At the design point of 500 ft/sec flow velocity, 3000°R aperture gas temperature, and 190 db sound pressure level, absorption coefficients are almost zero with either backing cavity. If these calculated values are correct, it must be concluded that the actual incident sound pressure level was much lower than 190 db. Note that fairly high values of absorption coefficients are obtained at the lower pressure levels, particularly with the 0.072-inch backing cavity.

CONCLUSIONS

Self-induced combustion instability and bomb-induced disturbances were successfully and consistently damped using the uncooled acoustic liner and both versions of the cooled liner.

No conclusions were reached regarding the theoretical value of the absorption coefficient required to damp the instability. The lack of a proven design procedure, plus the very significant effects of variations in design assumptions, makes the accurate calculation of the absorption coefficient almost impossible.

The half-length liner positioned in the injector end of the chamber was as effective in damping the instability as the full-length liner.

Resonator cavity gas temperatures were relatively low (1200°F), and no overheating of an uncooled copper outer chamber housing occurred during test durations to five seconds.

REFERENCES

1. Blackman, A. W.: Effect of Nonlinear Losses on the Design of Absorbers for Combustion Instabilities. ARS Journal, pp. 1022-1028, November 1960.

2. A Study of the Suppression of Combustion Oscillations with Mechanical Damping Devices. Phase II Summary Report, Pratt and Whitney Aircraft PWA FR-1922, July 15, 1966.

3. A Study of the Suppression of Combustion Oscillations with Mechanical Damping Devices. Quarterly Progress Report, Pratt and Whitney Aircraft PWA FR-2090, September 30, 1966.

4. A Study of the Suppression of Combustion Oscillations with Mechanical Damping Devices. Quarterly Progress Report, Pratt and Whitney Aircraft PWA FR-2247, December 30, 1966.

5. Ingard, U.: On the Theory and Design of Acoustic Resonators. Journ. Acoustical Soc. Amer., Volume 25, Number 6, pp. 1037-1061, November 1953.

APPENDIX

ACOUSTIC LINER SAMPLE CALCULATIONS

The following is a sample calculation of the absorption coefficient of the cooled acoustic liner at the first tangential frequency of the combustion chamber. Additional information and recommendations regarding calculation procedures are presented in references 2, 3, and 4. The configuration details and operating conditions are listed below:

ω_t = 7200 cps = 45,200 rad/sec
P_i = 190 db = 1,872 lb/ft^2 (assumed)
t = 0.20 in.
D_a = 0.04 in.
L = 0.169 in.
σ = 2.5% = 0.025
T_a = 2000°R (assumed)
μ_a = 0.34 x 10^{-4} lb/ft-sec
ρ_a = 1.05 lb/ft^3
C_a = 2280 ft/sec

The usual procedure is to first calculate the absorption coefficient assuming no-flow conditions, then to apply corrections to account for gas flow either past or through the apertures.

The absorption coefficient is given as:

$$\alpha = \frac{4\theta}{(\theta + 1)^2 + Q^2\theta^2 \left(\frac{\omega_t}{\omega_o} - \frac{\omega_o}{\omega_t}\right)^2} \tag{1}$$

where θ, the specific input resistance is:

$$\theta = \frac{R_d}{\sigma \rho_a C_a} \tag{2}$$

The resistance due to friction and turbulence is:

$$R_d = 2\sqrt{2 \mu_a \rho_a \omega_t} \quad (\epsilon + t/D_a) \tag{3}$$

where ϵ is the nonlinear resistance correction factor. The Blackman coorelation will be used for this analysis and may be read from Figure 13 or calculated from:

$$\epsilon = 1 + \sqrt{10\ (X_o/t)} \tag{4}$$

The ratio of particle displacement in the aperture to liner thickness, X_o/t, must be known before ϵ can be calculated. X_o is given as:

$$X_o = \frac{2\ P_i}{\left(\frac{\rho_a\ C_a{}^2\ \sigma}{L\ g}\right)} \left\{ \sqrt{\left[1 - \left(\frac{\omega t}{\omega_o}\right)^2\right]^2 + \left[\frac{(R_d + \sigma\ \rho_a\ C_a)\ \omega\ t}{\rho_a\ \ell_{ef}\ \omega_o{}^2}\right]^2} \right\}^{-1} \tag{5}$$

the effective length is equal to:

$$\ell_{ef} = \frac{t}{12} + 0.07\ D_a\ (1 - 0.7\ \sqrt{\sigma}) \tag{6}$$

$$\ell_{ef} = \frac{0.20}{12} + 0.07\ (0.040)\ (1 - 0.7\ \sqrt{.025})$$

$$\ell_{ef} = 0.0194 \text{ ft}$$

the resonant frequency is given as:

$$\omega_o = C_a \sqrt{\frac{\sigma}{L\ \ell_{ef}}} \tag{7}$$

$$\omega_o = 2280 \sqrt{\frac{.025\ (12)}{.169\ (.0194)}}$$

$$\omega_o = 21800 \text{ rad/sec}$$

Since equations (3), (4) and (5) are functions of each other, the calculation of R_d is an iteration process which is usually accomplished as follows:

First, estimate X_o from the following equation:

$$X_o' = \frac{2 P_i}{\left(\frac{\rho_a C_a^2 \sigma}{L g}\right)} \tag{8}$$

This value of X_o is used in equation (4) to calculate ϵ which, in turn, is used in equation (3) to calculate R_d. If this value of R_d satisfies equation (5) for the estimated value of X_o, the solution of R_d is complete. Otherwise, the process is repeated until a solution is obtained. The advantage of using a computer for this process should be evident.

Substituting known values in equation (8):

$$X_o' = \frac{2\ (1872)}{\frac{1.05\ (2280)^2\ (.025)}{.169\ (32.2)}}$$

$$X_o' = 0.149 \text{ in.}$$

$$\epsilon = 1 + \sqrt{10\ (X_o/t)}$$

$$\epsilon = 1 + \sqrt{10\ (0.149/0.20)}$$

$$\epsilon = 3.73$$

Substituting into equation (3):

$$R_d = 2\sqrt{2 \mu_a \rho_a \omega t} \qquad (\epsilon + t/D_a)$$

$$R_d = 2\sqrt{2(3.4 \times 10^{-5})\ (1.05)(4.52 \times 10^4)}\ \ (3.73 + 0.20/0.04)$$

$$R_d = 31.4$$

Substituting R_d into equation (5)

$$X_o = \frac{2(1872)}{\left[\frac{1.05(2280)^2(.025)}{.169(32.2)}\right]} \left(\frac{1}{\sqrt{\left[1 - \left(\frac{45200}{21800}\right)^2\right]^2 + \left\{\frac{[31.4 + 0.025(1.05)(2280)]\,45200}{1.05(0.0194)(21800)^2}\right\}^2}} \right)$$

$$X_o = 0.149 \left(\frac{1}{\sqrt{10.9 + .182}} \right)$$

$$X_o = 0.0447$$

This value differs significantly from the estimated value of X_o. The next step is to repeat the calculations using an assumed value of $X_o = 0.0447$, continuing the iteration until the equations are satisfied. The results of these calculations are:

$$R_d = 27.2$$

$$\epsilon = 2.51$$

$$X_o/t = 0.228$$

For the nonlinear resistance coorelations which are functions of sound pressure level rather than X_o/t, ϵ is read directly from the curves shown in Figure 13 and the iteration process is eliminated.

The specific input resistance, equation (2), is:

$$\theta = \frac{R_d}{\sigma\ \rho_a\ C_a}$$

$$\theta = \frac{27.2}{0.025(1.05)(2280)}$$

$$\theta = 0.454$$

The quality factor is:

$$Q = \frac{\omega_o \ell_{ef}}{\theta C_a \sigma} \tag{9}$$

$$Q = \frac{21800\,(.0194)}{0.454(2280)(0.025)}$$

$$Q = 16.3$$

Substituting into equation (1):

$$\alpha = \frac{4\theta}{(\theta + 1)^2 + Q^2\theta^2 \left(\frac{\omega_t}{\omega_o} - \frac{\omega_o}{\omega_t}\right)^2}$$

$$\alpha = \frac{4\,(0.454)}{(1.454)^2 + 16.3^2\,(0.454)^2 \left(\frac{45200}{21800} - \frac{21800}{45200}\right)^2}$$

$$\alpha = 1.3\ \%$$

The absorption coefficient for the same configuration will be made assuming a gas flow velocity of 500 ft/sec past the apertures. The procedure is similar to the no-flow calculations with modifications to correct for flow.

The shifted resonant frequency is calculated from

$$(\omega_o)_v = \omega_o\,(1 + \Delta f_o/f_o) \tag{10}$$

where $\Delta f_o/f_o$ is a constant 0.64 for velocities greater than 350 ft/sec.

$$(\omega_o)_v = 21800\ (1 + 0.64)$$

$$(\omega_o)_v = 35750$$

The effective length with flow is calculated from

$$(\ell_{ef})_v = \frac{12\ \sigma\ (C_a)^2}{L\ (\omega_o)_v^2}$$

$$(\ell_{ef})_v = \frac{12\ (.025)\ (2280)^2}{.169\ (35750)^2}$$

$$(\ell_{ef})_v = 0.00723 \text{ ft}$$

An iteration process similar to the one used in the no-flow case is used to calculate the resistance.

$$R_d = 2\sqrt{2\ \mu_a\ \rho_a\ \omega_o}\quad (\epsilon + t/D_a) \tag{11}$$

Note that ω_o is used for the flow case instead of ω_t.

The particle displacement equation is unchanged except for the two terms affected by flow velocity.

$$X_o = \frac{2\ P_j}{\left(\frac{\rho_a\ C_a\ \sigma}{L\ g}\right)} \left(\frac{1}{\sqrt{\left\{ 1 - \left[\frac{\omega_t}{(\omega_o)_v}\right]^2 \right\}^2 + \left[\frac{(R_d + \sigma\ \rho_a\ C_a)\ \omega_t}{\rho_a\ (\ell_{ef})_v\ (\omega_o)_v^2}\right]^2}} \right) \tag{12}$$

Both equation (4) and (8) are unchanged.

The following values were calculated by iteration:

$$R_d = 23.2$$

$\epsilon = 4.27$

$X_o/t = 1.068$

The specific resistance with flow past the apertures is given as:

$$\theta_v = \frac{R_d}{\sigma \rho_a C_a} \quad (1 - A_f V)^{-4} \tag{13}$$

where A_f is an amplitude parameter having a constant value of 0.67×10^{-3} for all frequencies greater than 2000 cps.

$$\theta_v = \frac{23.2}{0.025\ (1.05)\ (2280)} \quad [1 - (0.67 \times 10^{-3})(500)]^{-4}$$

$\theta_v = 1.98$

$$Q_v = \frac{(\omega_o)_v\ (\ell ef)_v}{C_a\ \sigma\ \theta_v}$$

$$Q_v = \frac{35750\ (7.23 \times 10^{-3})}{2280\ (.025)\ (1.98)}$$

$Q_v = 2.28$

Substituting the values corrected for flow into equation (1):

$$\alpha = \frac{4\ \theta_v}{(\theta_v + 1)^2 + Q_v^2\ \theta_v^2 \left[\frac{\omega_t}{(\omega_o)_v} - \frac{(\omega_o)_v}{\omega_t}\right]^2}$$

$$\alpha = \frac{4\ (1.98)}{(1.98 + 1)^2 + (2.28)^2\ (1.98)^2 \left(\frac{45200}{35750} - \frac{35750}{45200}\right)^2}$$

$\alpha = 59\ \%$

TABLE I

PERFORMANCE DATA

RUN No.	P_c psia	W_f lb/sec	W_o lb/sec	W_o/W_f	F lb	t sec	η_c* %	T_1 °F	T_2 °F	
147-25	995	3.81	10.44	2.70	3690	2.0	92.0	—	—	Base instability firing. No acoustic liner
147-48	1031	4.68	9.55	2.04	3690	3.0	93.5	—	—	Uncooled Liner Test - Liner destroyed
147-67	1018	5.17	9.97	1.93	3820	3.0	92.5	—	—	Uncooled Liner Test - Liner destroyed
176-1	966	—	—	3.07	3500	1.2	—	—	—	First firing of cooled liner test series. Stable combustion
176-2	1032	5.41	9.18	1.70	3692	3.0	96.5	1012	828	No backing spacer. Full length liner
176-3	1014	4.62	10.07	2.20	3642	3.0	90.0	1102	890	Same as -2
176-4	1009	4.45	9.97	2.20	3600	3.0	91.0	1217	1116	Same as -2
176-5	1018	4.93	9.67	1.96	3657	3.0	91.2	938	No Good	Backing Spacer used. Full length liner
176-6		NO	DATA							Test aborted due to TEA leak
176-7	1012	4.95	9.74	1.97	3686	5.0	91.8	1136	No Good	No backing spacer. Half-length liner
176-8	1016	5.12	9.46	1.85	3700	3.0	91.5	1031	No Good	Same as -7
176-9	1021	4.77	9.99	2.09	3700	1.9	92.0	1034	819	Same as -7 plus 6.9 grain bomb test
176-10	1019	4.97	10.05	2.01	3706	5.0	90.4	1139	No Good	Backing spacer used. Half-length liner. 6.9 grain bomb test.
176-11	1042	4.91	10.27	2.09	3809	4.6	91.0	1443 max.	No Good	Backing spacer used. Half-length liner. 13.5 grain bomb test
176-12	952	4.90	9.58	1.96	3887	1.3	90.5	—	—	Base instability firing. No acoustic liner

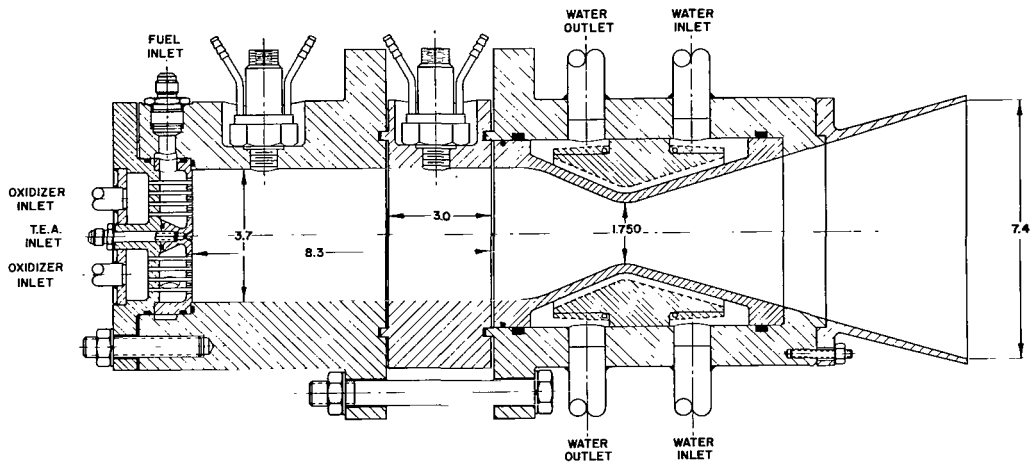

(a) Basic Thrust Chamber

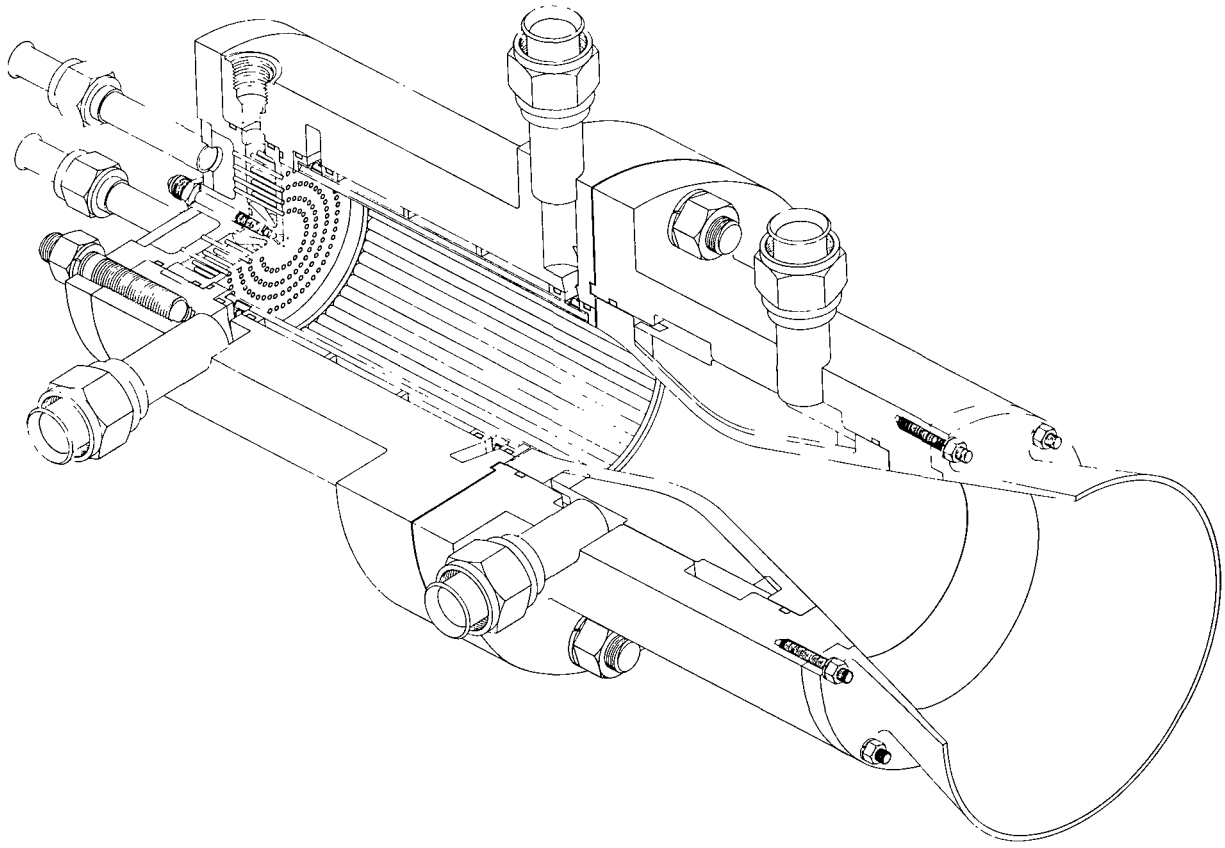

(b) Cooled Acoustic Liner Configuration

FIG. 1 THRUST CHAMBER ASSEMBLY

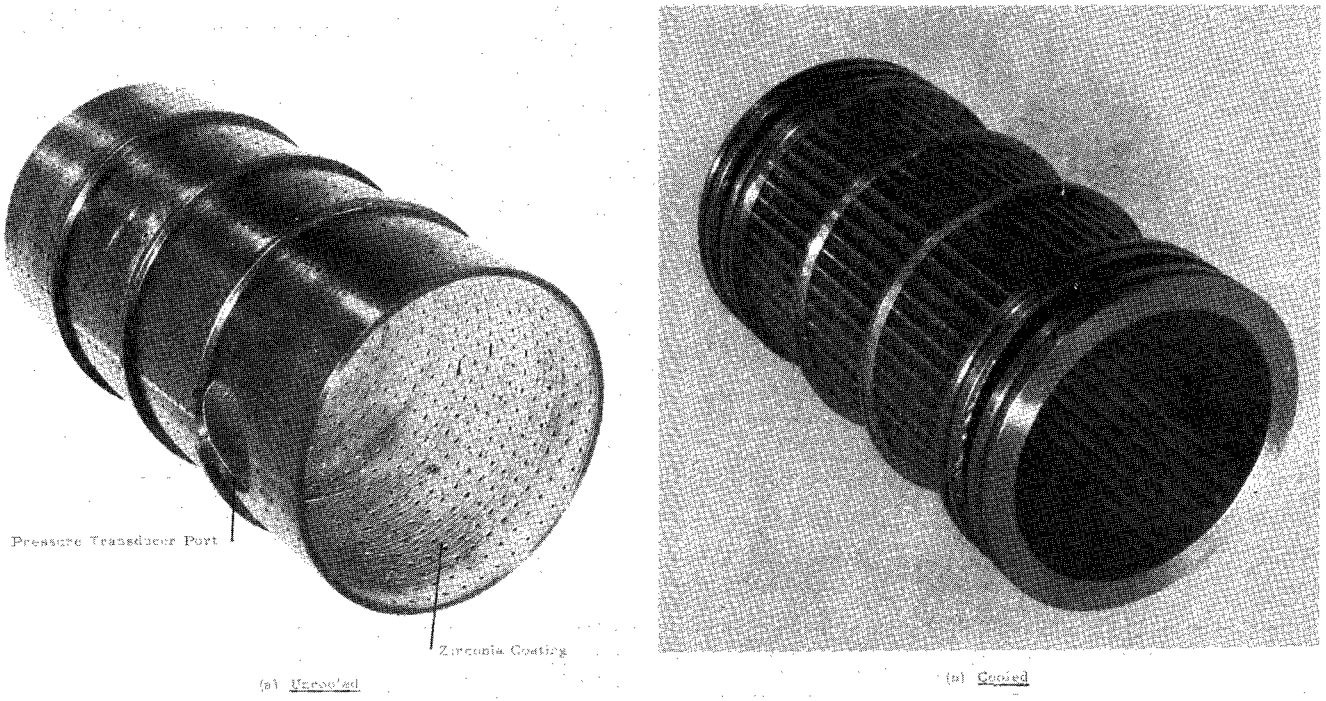

FIG. 2 ACOUSTIC CHAMBER LINER

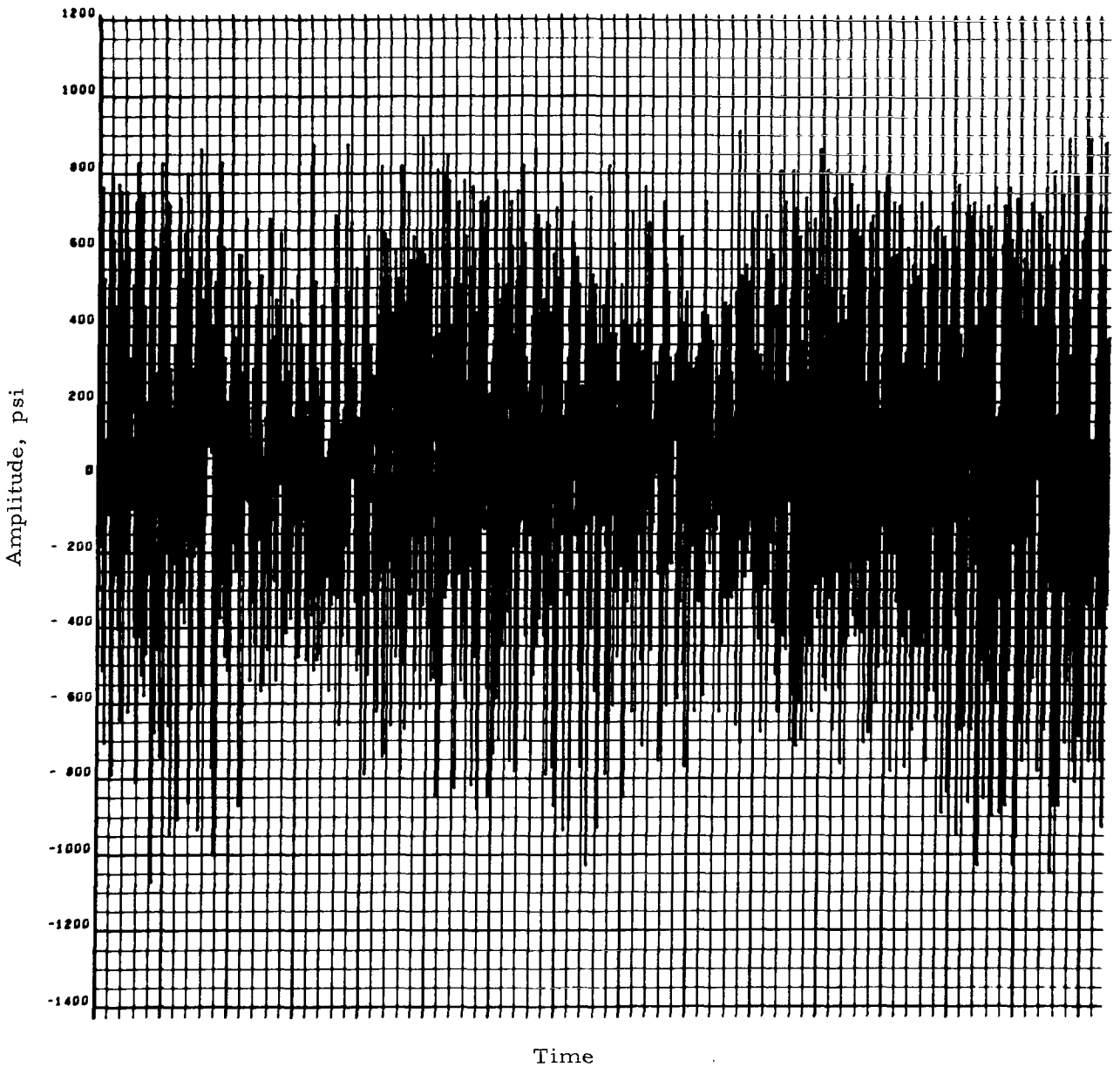

FIG. 3 INSTABILITY PRESSURE AMPLITUDES, DIGITIZED DATA, RUN 147-25

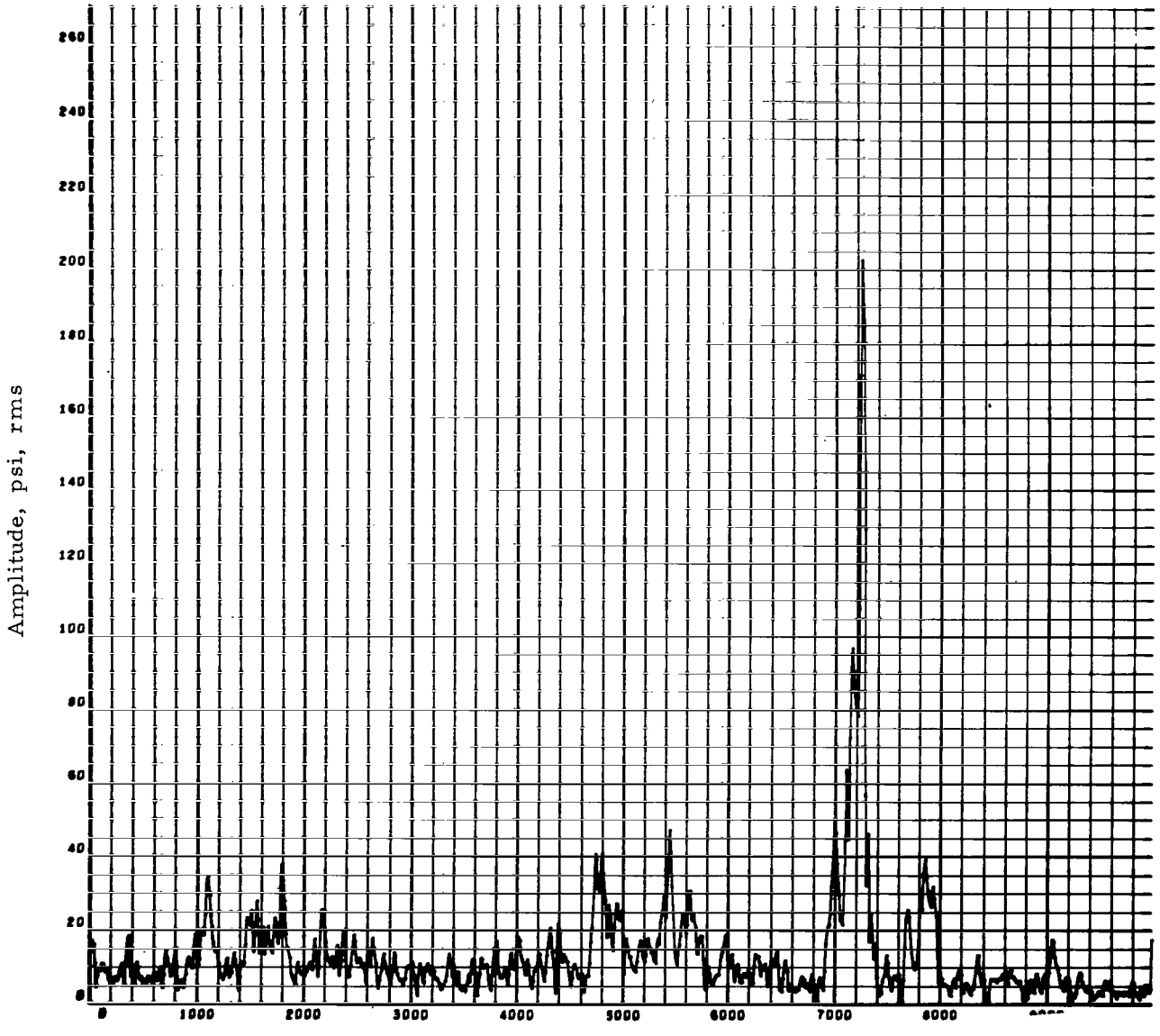

FIG. 4 FREQUENCY ANALYSIS, RUN 147-25

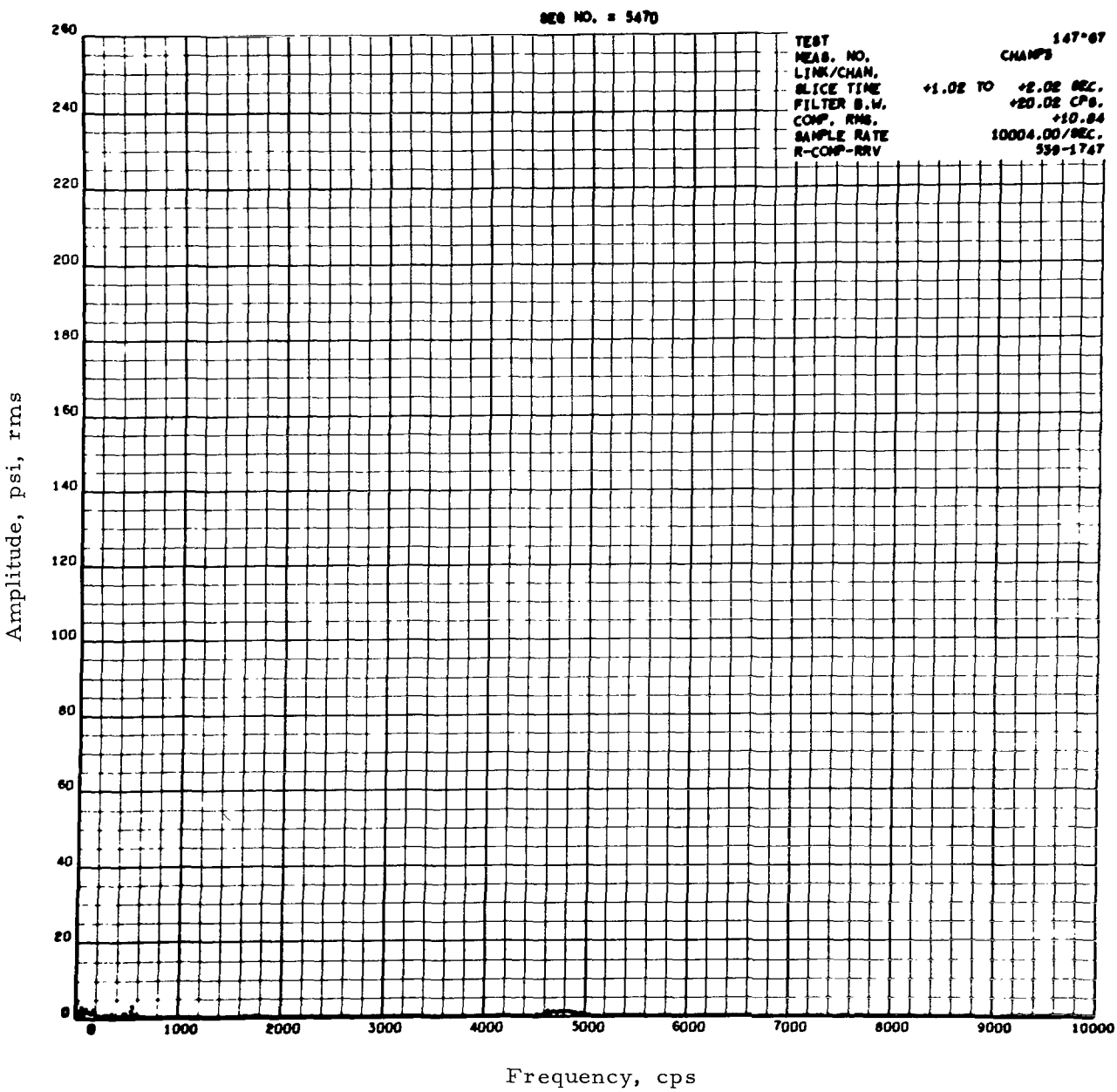

FIG. 5 FREQUENCY ANALYSIS, RUN 147-67

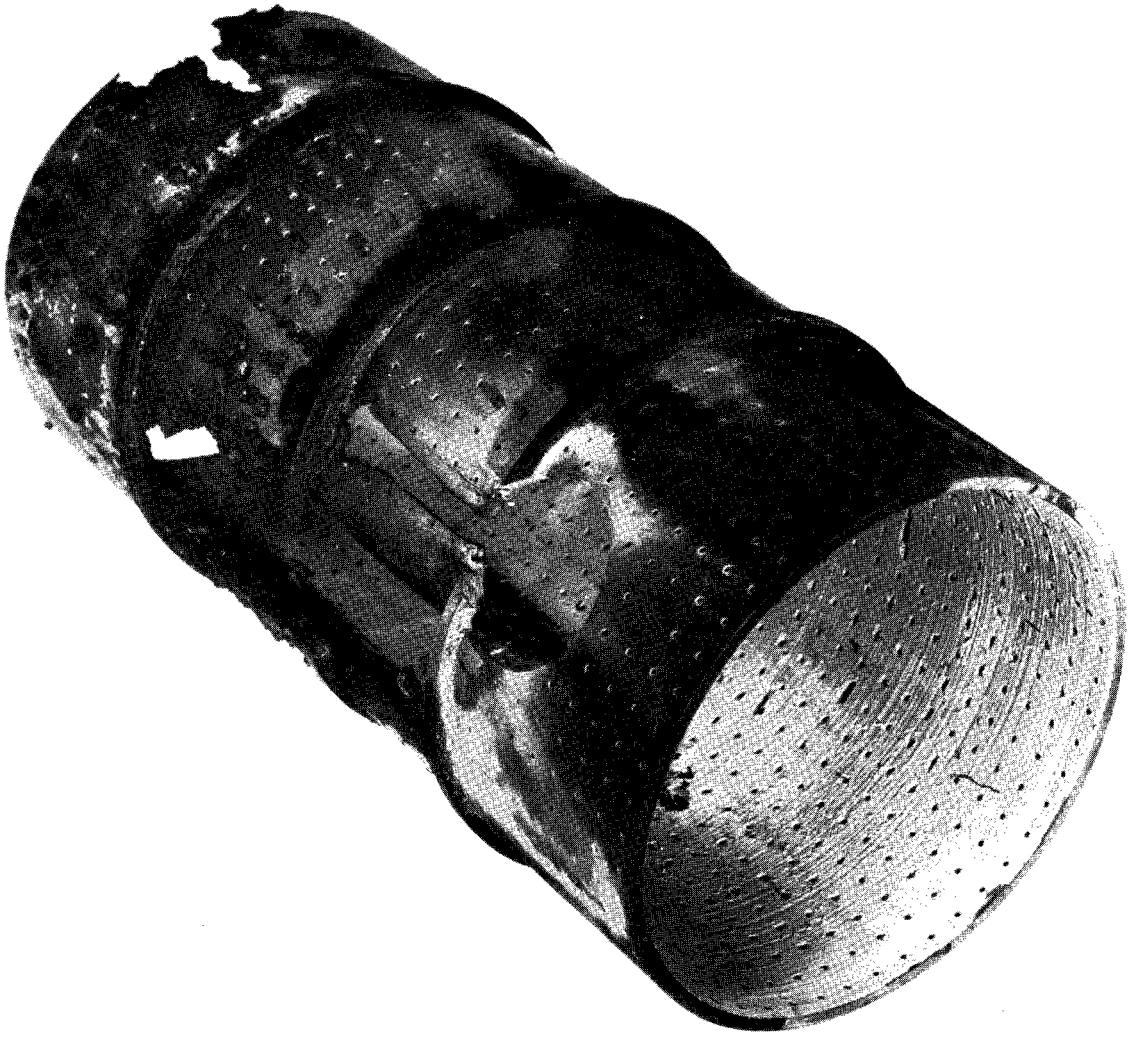

FIG. 6 UNCOOLED LINER AFTER ONE 3-SECOND FIRING

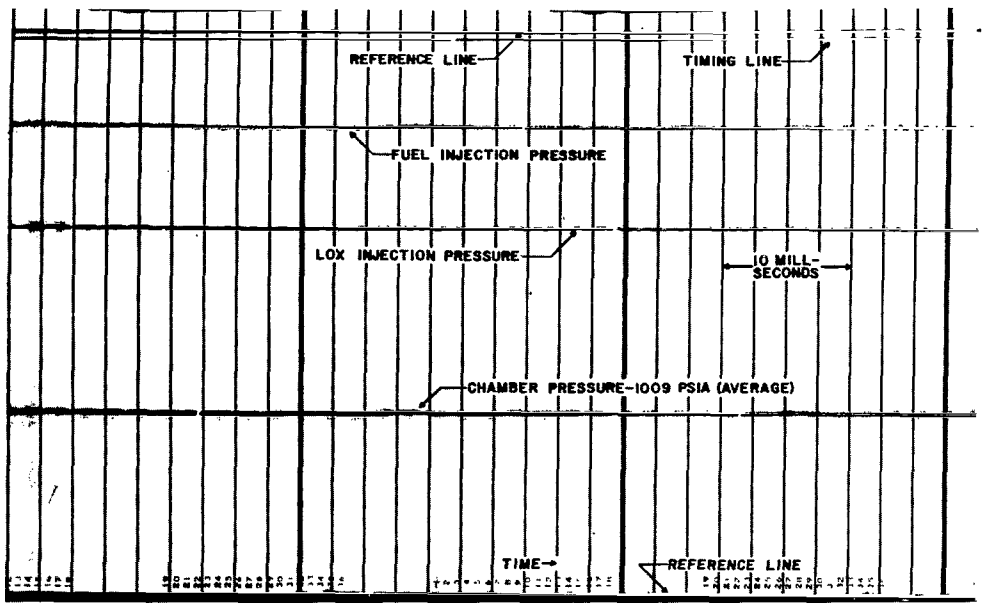

Test Number 176-4

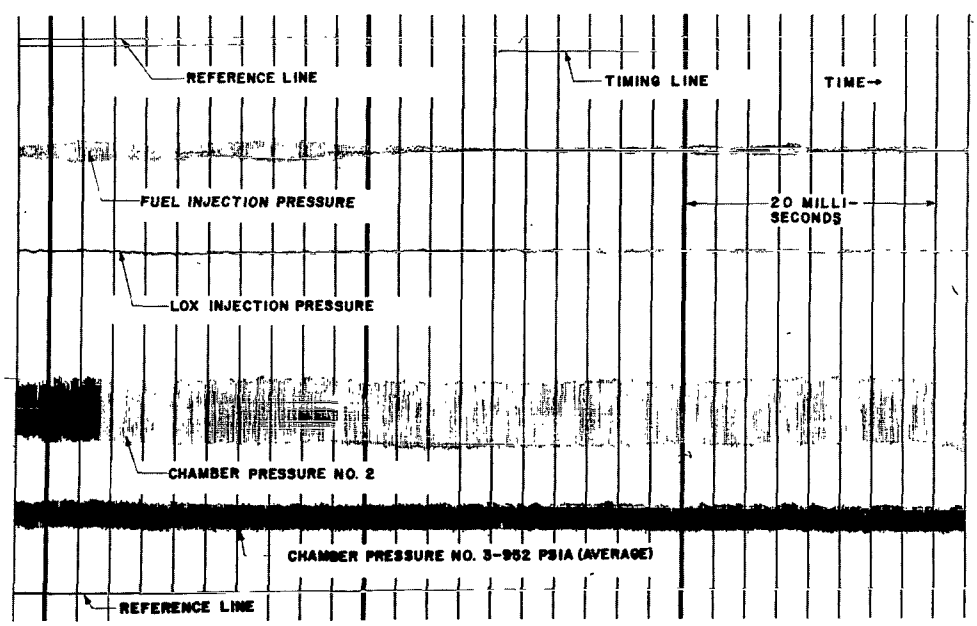

Test Number 176-12

FIG. 7 OSCILLOGRAMS FOR FIRINGS WITH AND WITHOUT ACOUSTIC LINERS

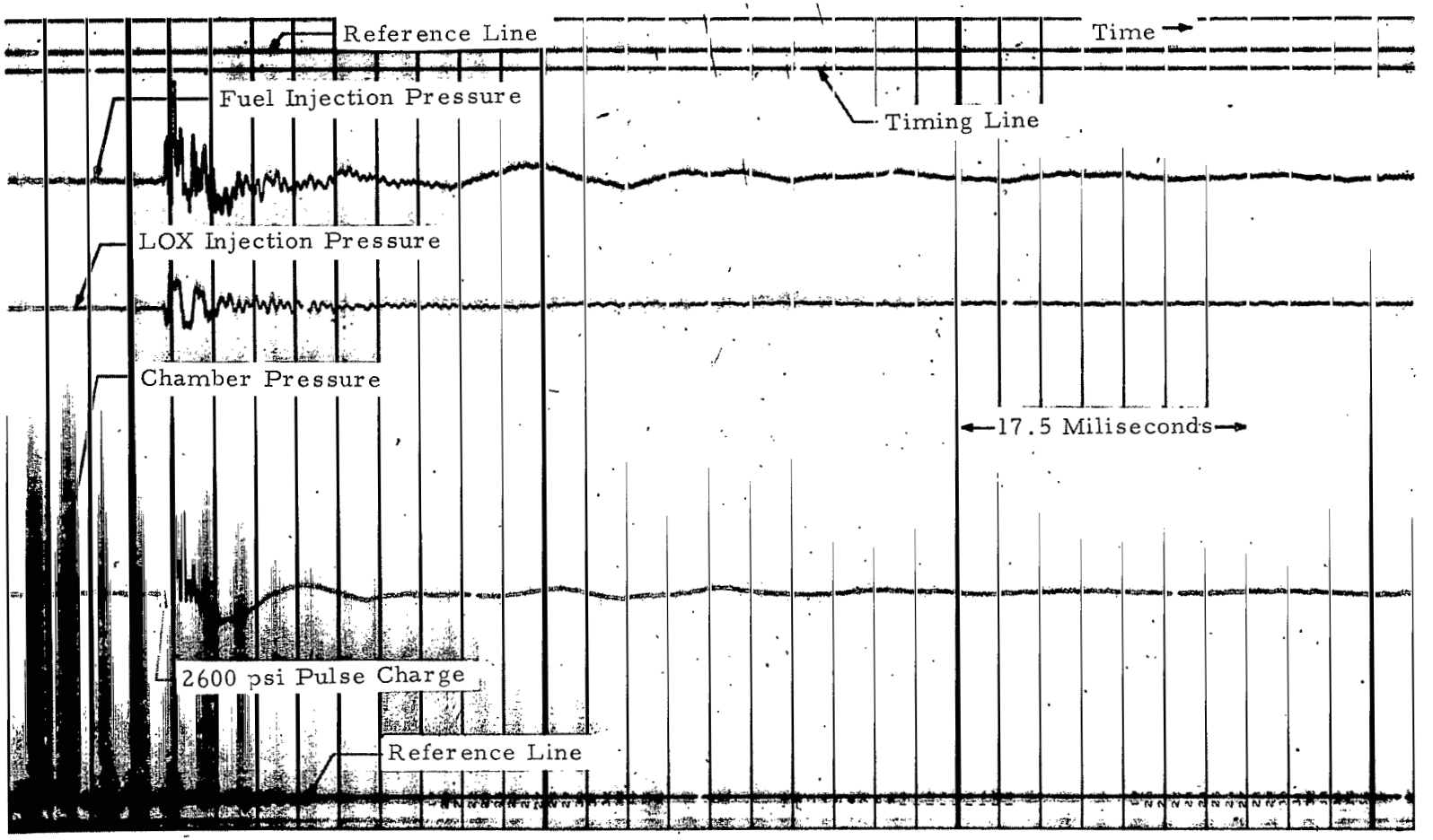

FIG. 8 OSCILLOGRAM OF 13.5 GRAIN CHARGE
PULSING THE ACOUSTIC-LINER CHAMBER, RUN 176-11

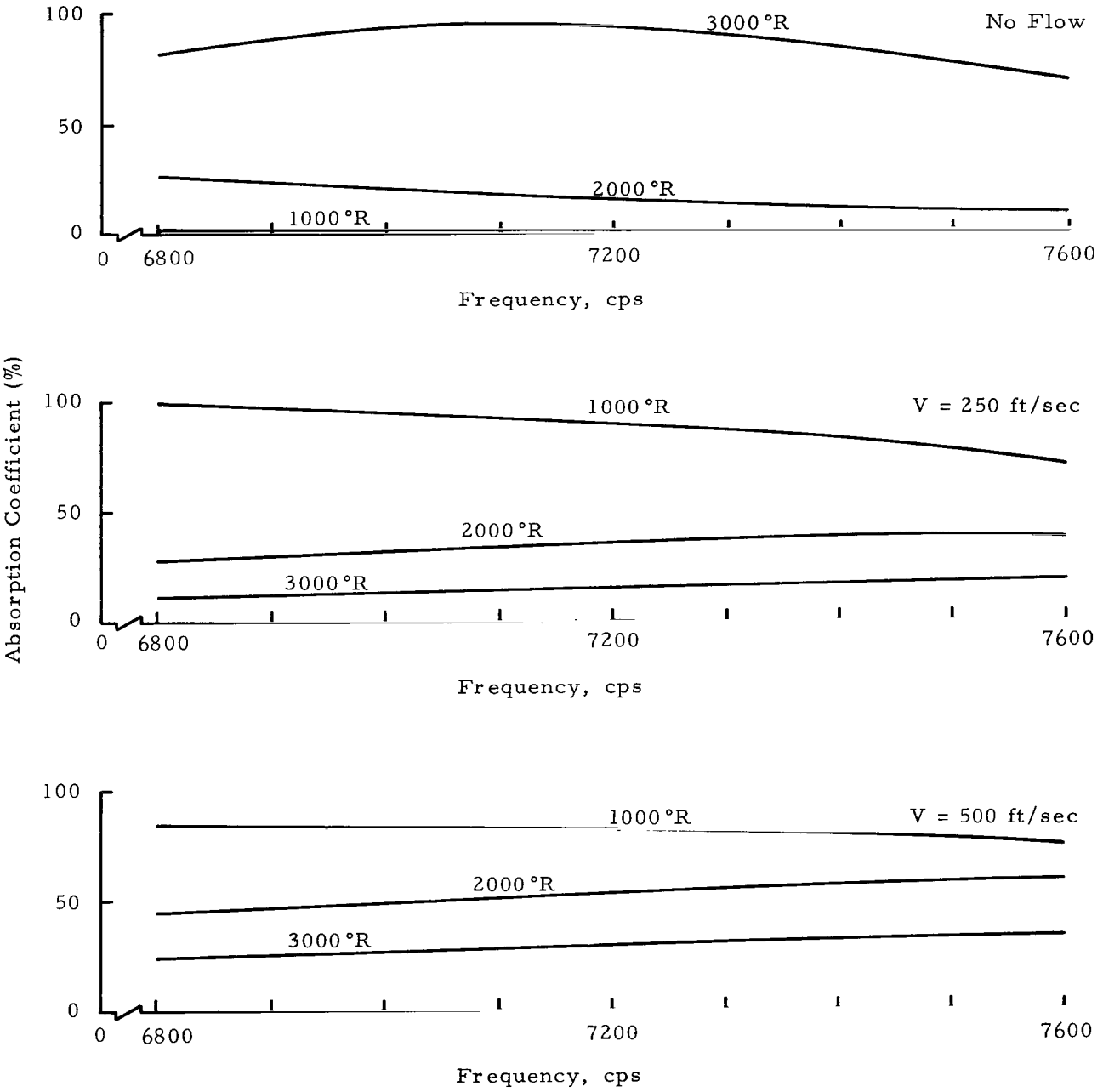

FIG. 9 VARIATIONS IN ABSORPTION COEFFICIENTS WITH DESIGN ASSUMPTIONS, UNCOOLED LINER

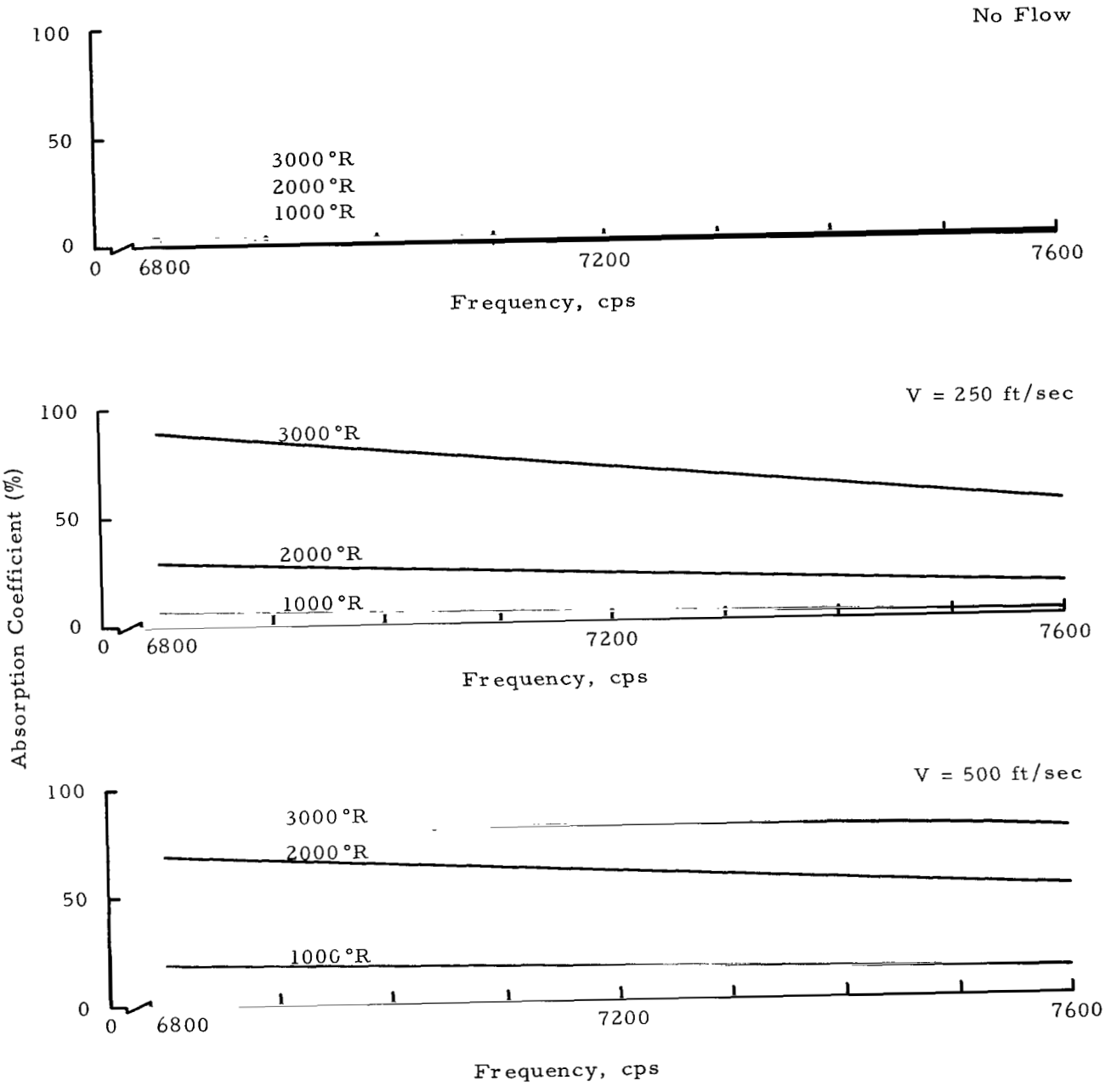

FIG. 10 VARIATIONS IN ABSORPTION COEFFICIENTS WITH DESIGN ASSUMPTIONS, COOLED LINER, 0.169 inch Backing Cavity

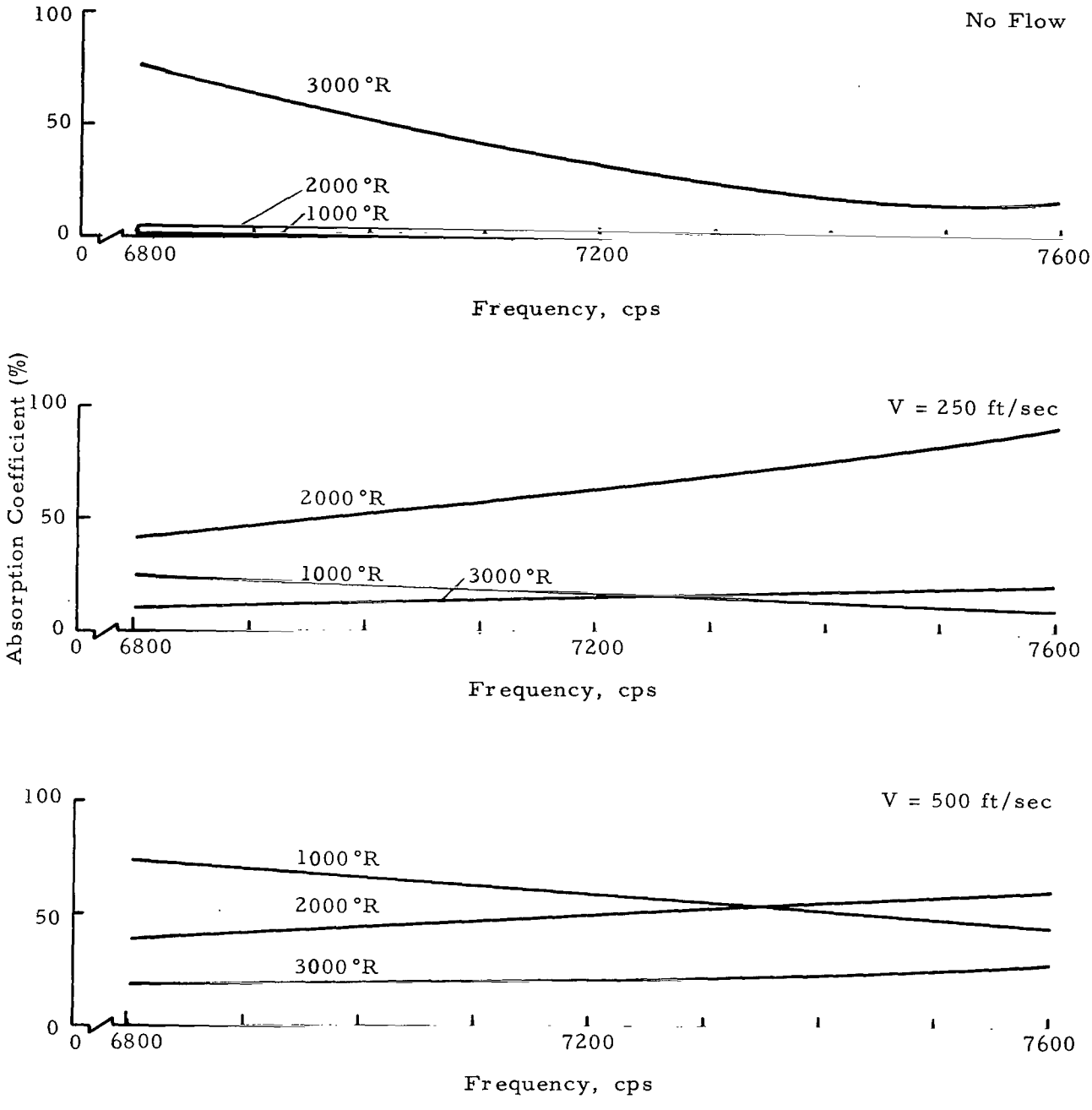

FIG. 11 VARIATIONS IN ABSORPTION COEFFICIENTS WITH DESIGN ASSUMPTIONS, COOLED LINER, 0.072 inch Backing Cavity

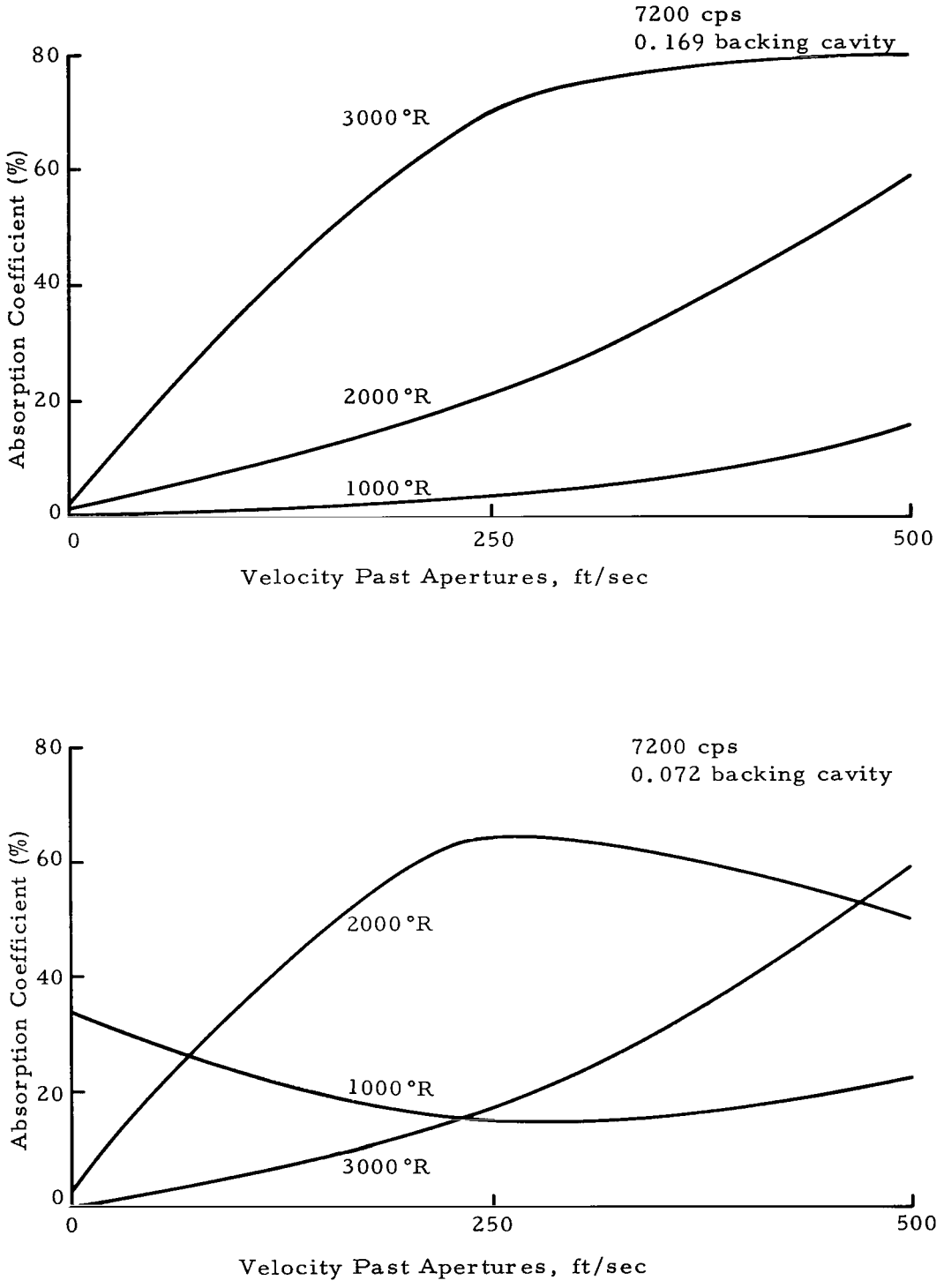

FIG. 12 EFFECTS OF APERTURE GAS TEMPERATURE AND FLOW PAST APERTURES ON ABSORPTION COEFFICIENTS, COOLED LINERS

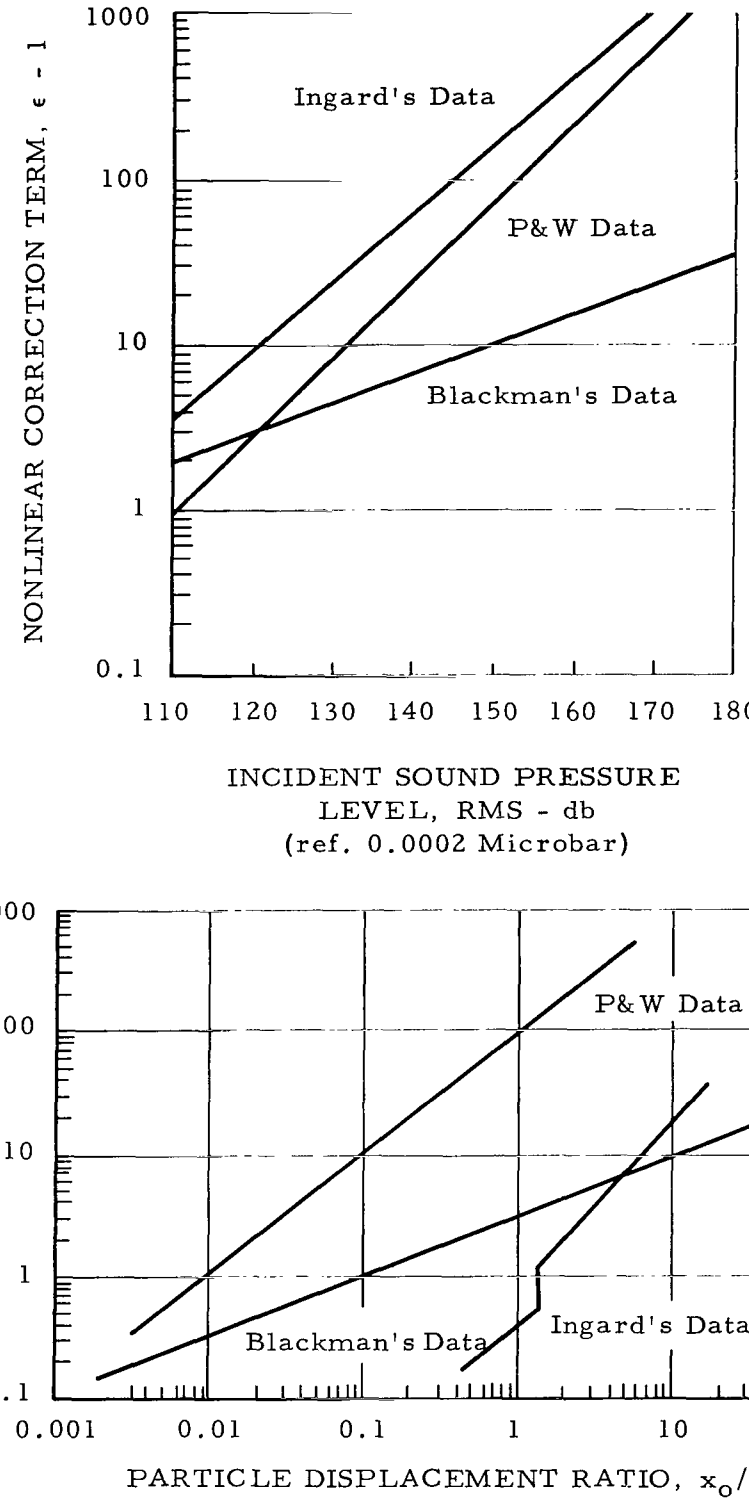

FIG. 13 NONLINEAR RESISTANCE CORRELATIONS AS FUNCTIONS OF INCIDENT SOUND PRESSURE LEVEL AND PARTICLE DISPLACEMENT RATIO

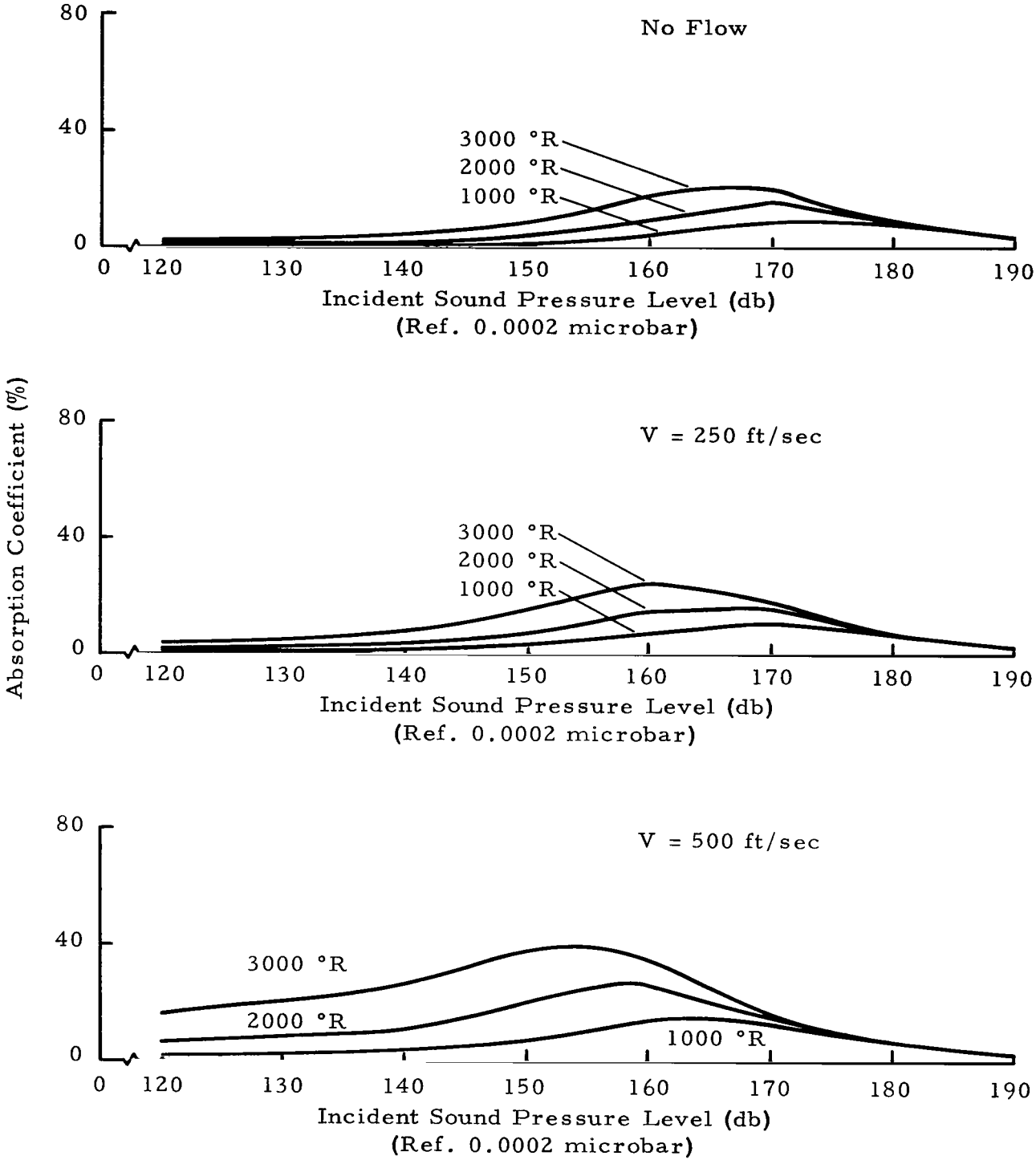

FIG. 14 ABSORPTION COEFFICIENT VERSUS INCIDENT SOUND PRESSURE LEVEL, 7200 cps, 0.169 Backing Cavity, COOLED LINER, PRATT AND WHITNEY NONLINEAR CORRECTION

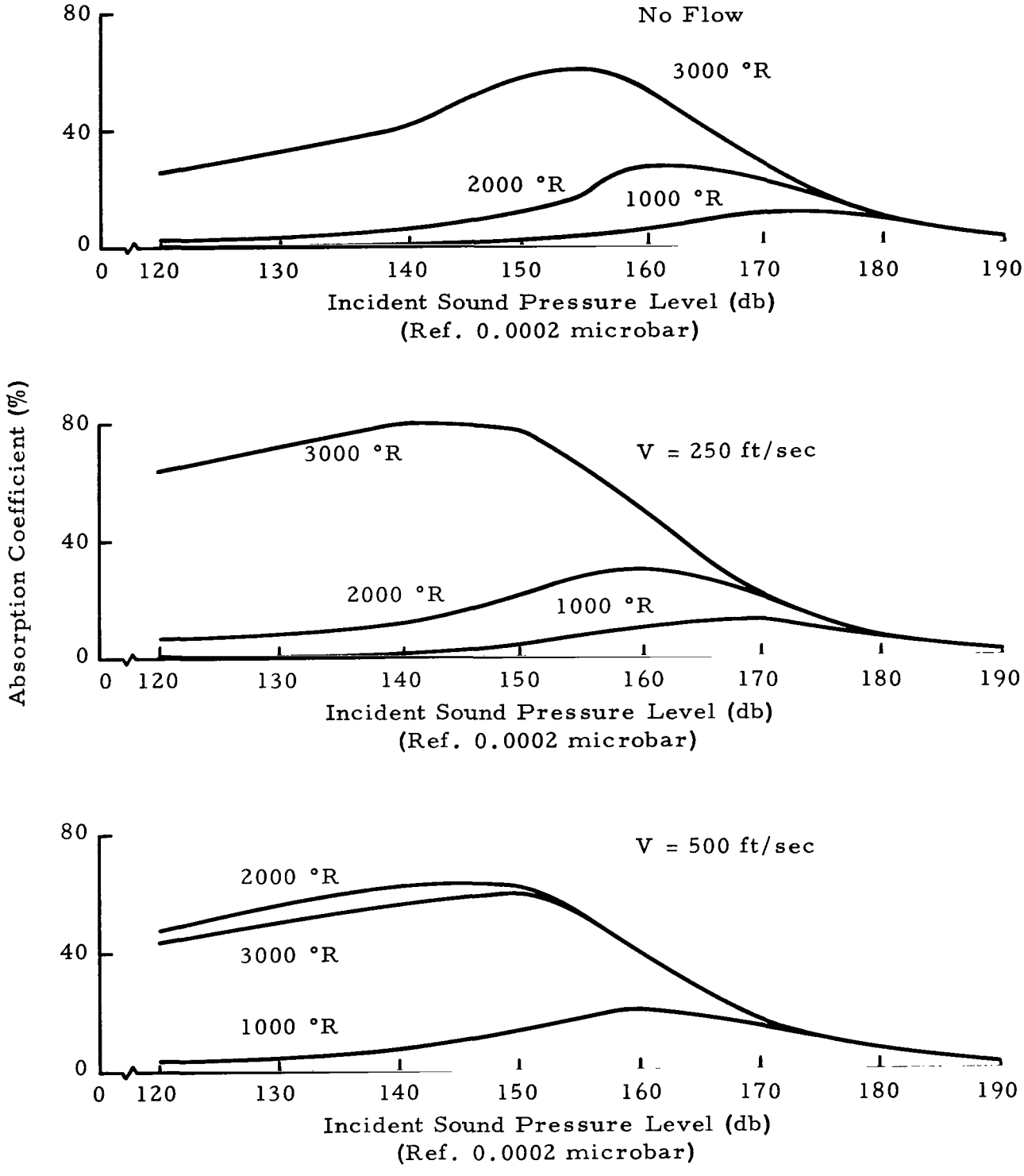

FIG. 15 ABSORPTION COEFFICIENT VERSUS INCIDENT SOUND PRESSURE LEVEL, 7200 cps, 0.072 Backing Cavity, COOLED LINER, PRATT AND WHITNEY NONLINEAR CORRECTION

NASA-Langley, 1967 — 28 M348

"The aeronautical and space activities of the United States shall be conducted so as to contribute . . . to the expansion of human knowledge of phenomena in the atmosphere and space. The Administration shall provide for the widest practicable and appropriate dissemination of information concerning its activities and the results thereof."

—NATIONAL AERONAUTICS AND SPACE ACT OF 1958

NASA SCIENTIFIC AND TECHNICAL PUBLICATIONS

TECHNICAL REPORTS: Scientific and technical information considered important, complete, and a lasting contribution to existing knowledge.

TECHNICAL NOTES: Information less broad in scope but nevertheless of importance as a contribution to existing knowledge.

TECHNICAL MEMORANDUMS: Information receiving limited distribution because of preliminary data, security classification, or other reasons.

CONTRACTOR REPORTS: Scientific and technical information generated under a NASA contract or grant and considered an important contribution to existing knowledge.

TECHNICAL TRANSLATIONS: Information published in a foreign language considered to merit NASA distribution in English.

SPECIAL PUBLICATIONS: Information derived from or of value to NASA activities. Publications include conference proceedings, monographs, data compilations, handbooks, sourcebooks, and special bibliographies.

TECHNOLOGY UTILIZATION PUBLICATIONS: Information on technology used by NASA that may be of particular interest in commercial and other non-aerospace applications. Publications include Tech Briefs, Technology Utilization Reports and Notes, and Technology Surveys.

Details on the availability of these publications may be obtained from:

SCIENTIFIC AND TECHNICAL INFORMATION DIVISION

NATIONAL AERONAUTICS AND SPACE ADMINISTRATION

Washington, D.C. 20546